SUPPLEMENTARY FIGURES AND DATA

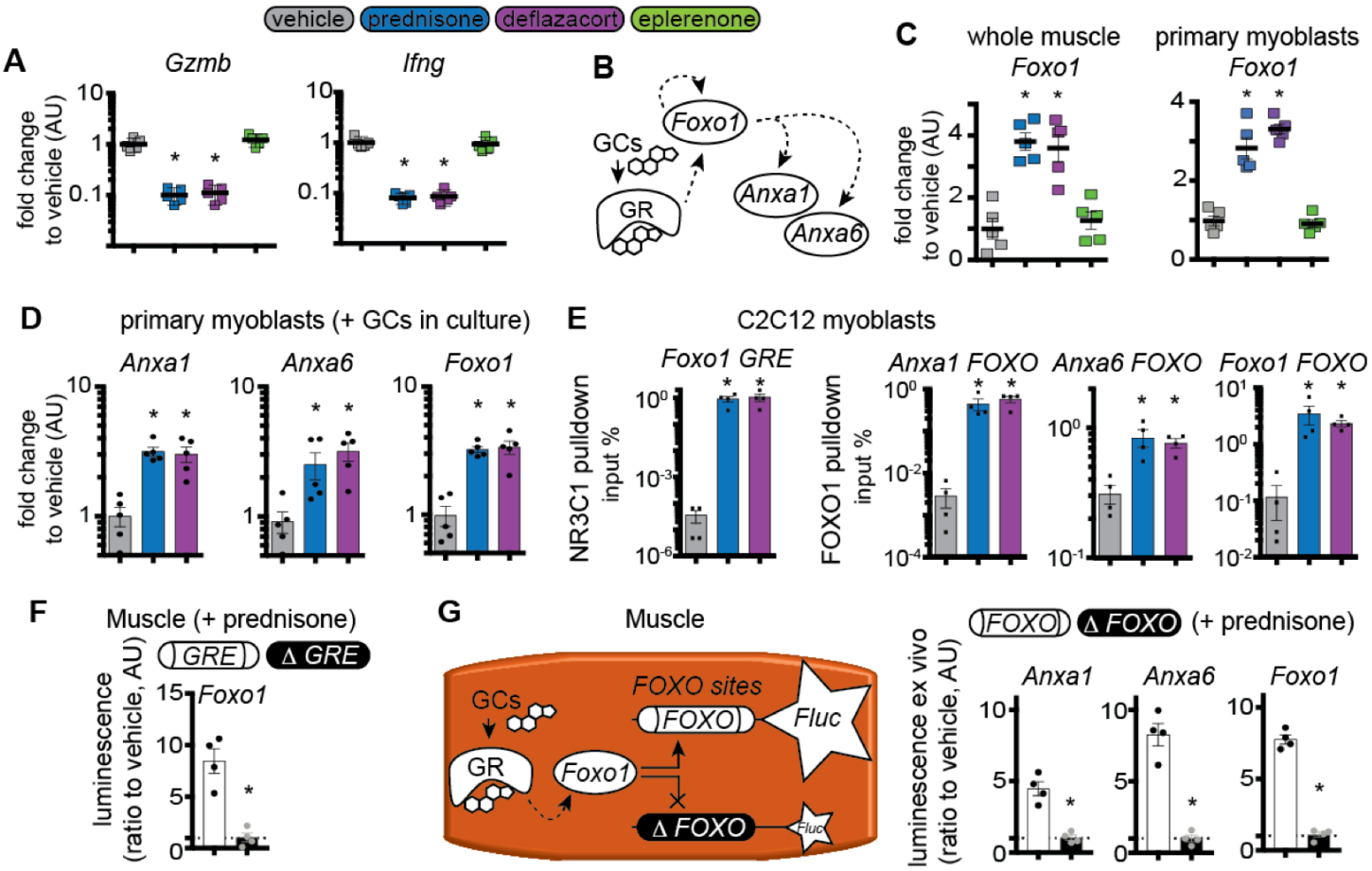

Supplementary Figure 1. GC pulse induces *Foxo1* upregulation, which reinforces upregulation of *Anxa1* and *Anxa6*. A) GC steroid uptake was confirmed by reduced expression of immune system activation markers in splenocytes. **B)** Model of transactivation pathway linking GCs in muscle to regulation of *Anxa1* and *Anxa6* by *Foxo1*; dashed lines, interrogated interactions. **C)** *Foxo1* was upregulated in skeletal muscle (quadriceps) and primary myoblasts (tibialis anterior) of mice 24 hours after a single pulse of GC steroids. **D)** 24 hours after treating GC with steroids in culture expression of *Anxa1*, *Anxa6*, and *Foxo1* was upregulated in wildtype primary myoblasts (from tibialis anterior), as compared to vehicle. **E)** 24 hours after a single GC pulse in C2C12 cells, ChIP-qPCR analysis showed that the *Foxo1 GRE* site was significantly enriched in GR occupancy. The FOXO sites of *Anxa1*, *Anxa6*, and *Foxo1* were also increased in FOXO1 occupancy, as compared to vehicle. **F)** Prednisone pulse in vivo upregulated luciferase activity of reporter constructs either containing or deleted for the *Foxo1 GRE* site. **G)** *(left)* Diagram depicting experimental design for testing FOXO sites in muscle using electroporation of constructs into muscles. 24 hours after i.p. prednisone pulse in wildtype mice luciferase activity when constructs contained the FOXO sites (white bars). Conversely, GC-related upregulation was ablated after deletion of the binding site in the constructs (black bars). **(E-F)** Data are expressed as fold change to luminescence from vehicle-treated FDB muscles electroporated with the same plasmids (dashed line n=5 mice/group **(B-C)**; n=4 assays or mice/group **(D-F)**. *, P<0.05 vs vehicle, 1-way ANOVA test with Bonferroni multiple comparison **(B-D)**; *, P<0.05 vs wildtype site construct, unpaired two-tailed t-test with Welch's correction **(E-F)**.

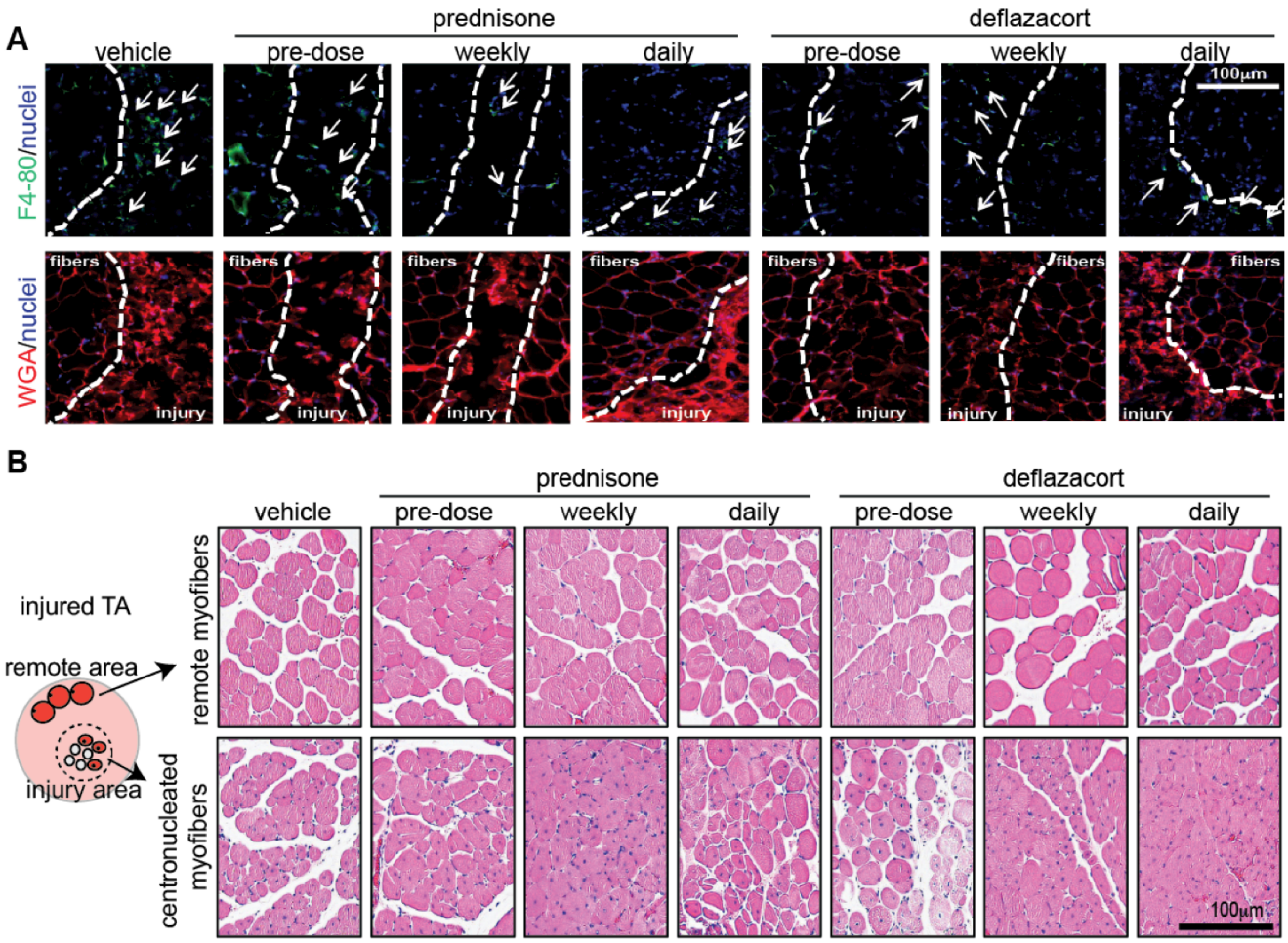

Supplemental Figure 2. Both daily and weekly GC treatment reduced the extent of injury and fibrosis, but daily GC dosing induced features of atrophy. WT *gastrocnemius* muscles were injured with cardiotoxin injection and imaged 7 days after injury. **A)** All GC treatments decreased macrophage infiltrates within area of injury. WGA (lowel panels, red) identifies the regions of injury with dashed white lines demarcating the edge of injury. F4-80+ macrophages (green, upper panels; arrows) cluster within the injury area and towards the edge of the region of injury. **B)** Weekly GC treatment associated with increased CSA of intact myofibers remote from the injury site, while daily dosing correlated with decreased CSA values in remote fibers in *tibialis anterior*. These trends were not observed in areas with centrally-nucleated myofibers which marks the injury area itself. n=6 mice/group.

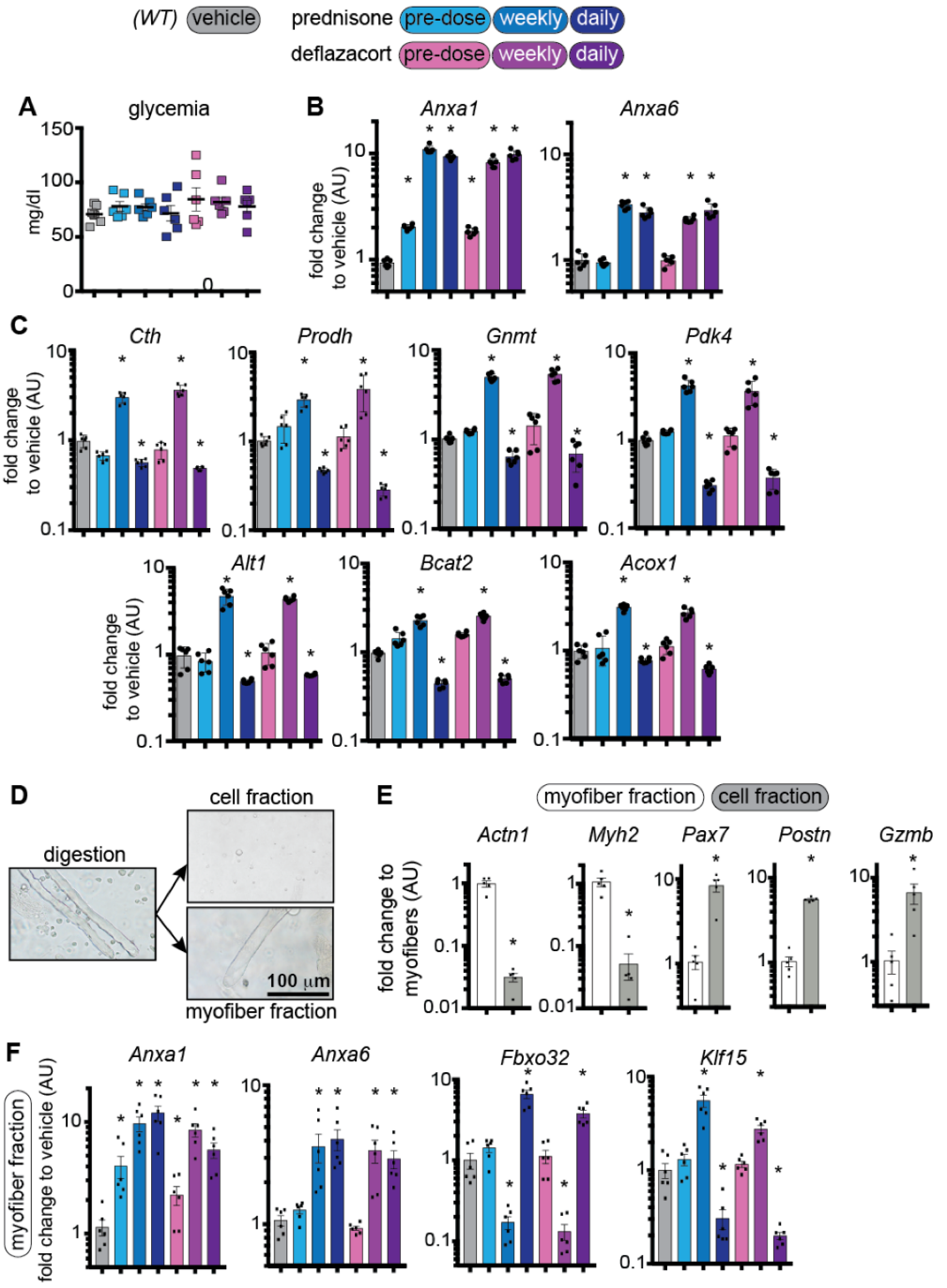

Supplementary Figure 3. Response to GC steroid dosing in WT mice. **A)** No significant changes were observed in serum glucose with either weekly or daily GC steroid dosing. **B)** *Anxa1* and *Anxa6* are increased in *tibialis anterior* muscles after weekly and daily treatments. **C)** Genes downstream of the KLF15 metabolic pathway demonstrate a similar pattern to *Klf15* after steroid treatment regimens. Dot plots, single mouse values; histograms, single values and avg±sem; n=6 mice/group; *, P<0.05 vs vehicle, 1-way ANOVA test with Bonferroni multiple comparison. **D)** Representative brightfield pictures showing separation of mononuclear- and myofiber-fractions from whole muscle digestion (5 replicates). **E)** qPCRs validation with markers differentiating the myofiber (sarcomeric markers) and the mononuclear fractions (*Pax7*, satellite cells; *Postn*, myofibroblasts; *Gzmb*, immune cells). **F)** qPCR analysis of the myofibers fraction from *tibialis anterior* muscle after GC treatments demonstrated the same pattern as seen in whole muscle. n=6 mice/group **(ABC)**; n=5 mice/group **(EF)**; *, P<0.05 vs vehicle, 1-way ANOVA test with Bonferroni multiple comparison **(A-C, F)**. *, P<0.05 vs myofiber fraction, t-test with Welch's correction **(E)**.

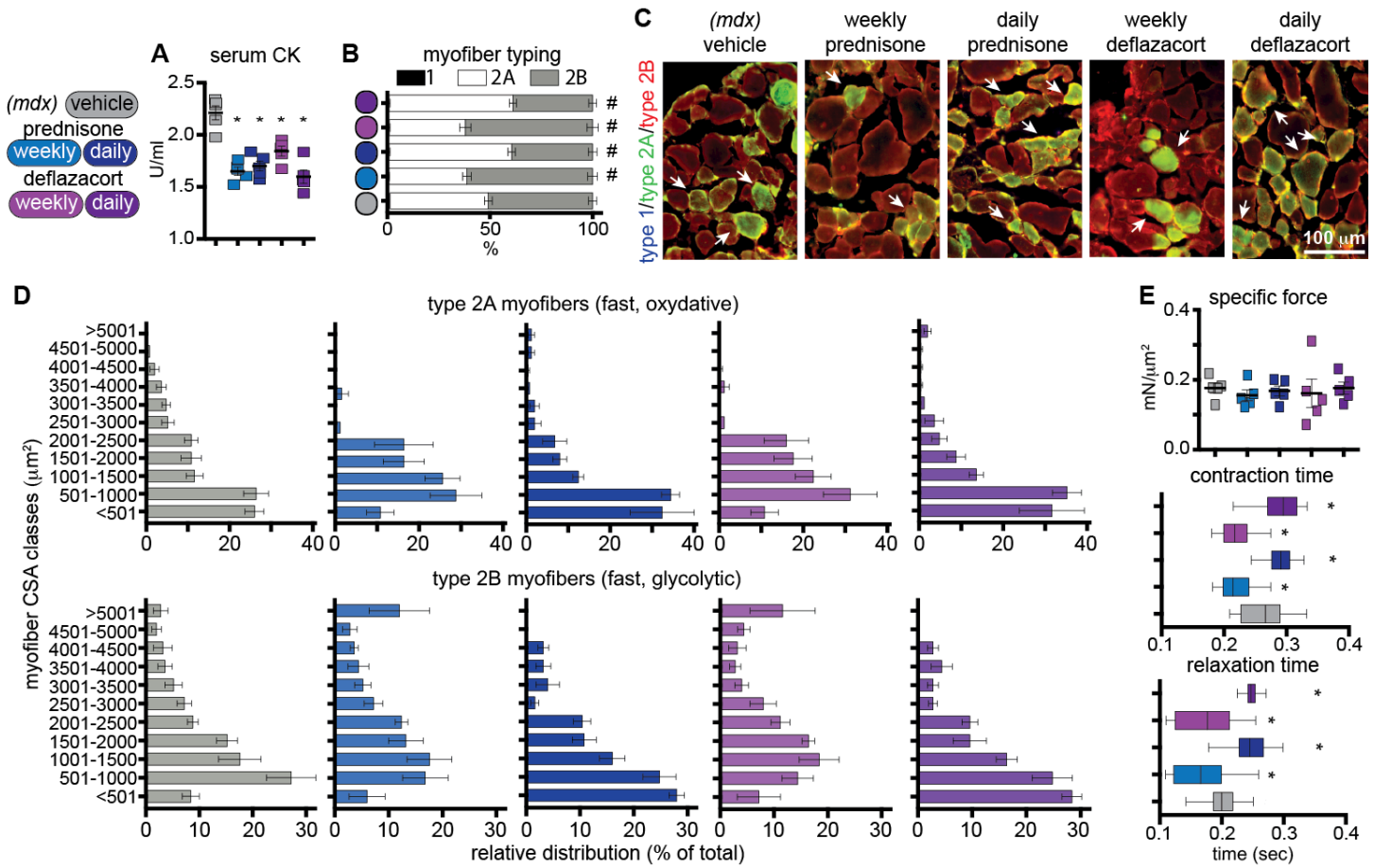

Supplementary Figure 4. Regimen-specific effects on serum CK, myofiber type, specific force, and contraction/relaxation times of treated *mdx* muscles. A) Serum CK was comparably reduced by all GC regimens after 4-week treatment. **B-C)** Fast glycolytic fibers (type 2B) were increased after weekly treatments, while fast oxidative fibers (type 2A) were increased after daily treatment, as revealed by *quadriceps* section immunostaining (representative pictures shown in **C;** 10 replicates). **D)** Myofiber CSA class distribution of type 2A myofibers show a relative increase in small (<501mm2) fast oxidative myofibers after daily GC regimens, as compared to vehicle and weekly treated. Conversely, weekly GC regimens associated with a relative increase in large type 2B myofibers (>5001mm2), as compared to vehicle and daily treated (global changes in CSA class distribution not significant with 2-way ANOVA test). **E)** Tibialis anterior specific force did not significantly change with regards to GC regimen type. Conversely, contraction and relaxation were faster after weekly GC treatment, and slower after daily GC regimen than after vehicle treatment. n=5 mice/group; *****, P<0.05 vs vehicle, 1-way ANOVA test with Bonferroni multiple comparison; **#**, P<0.05 vs vehicle, 2-way ANOVA test with Bonferroni multiple comparison.

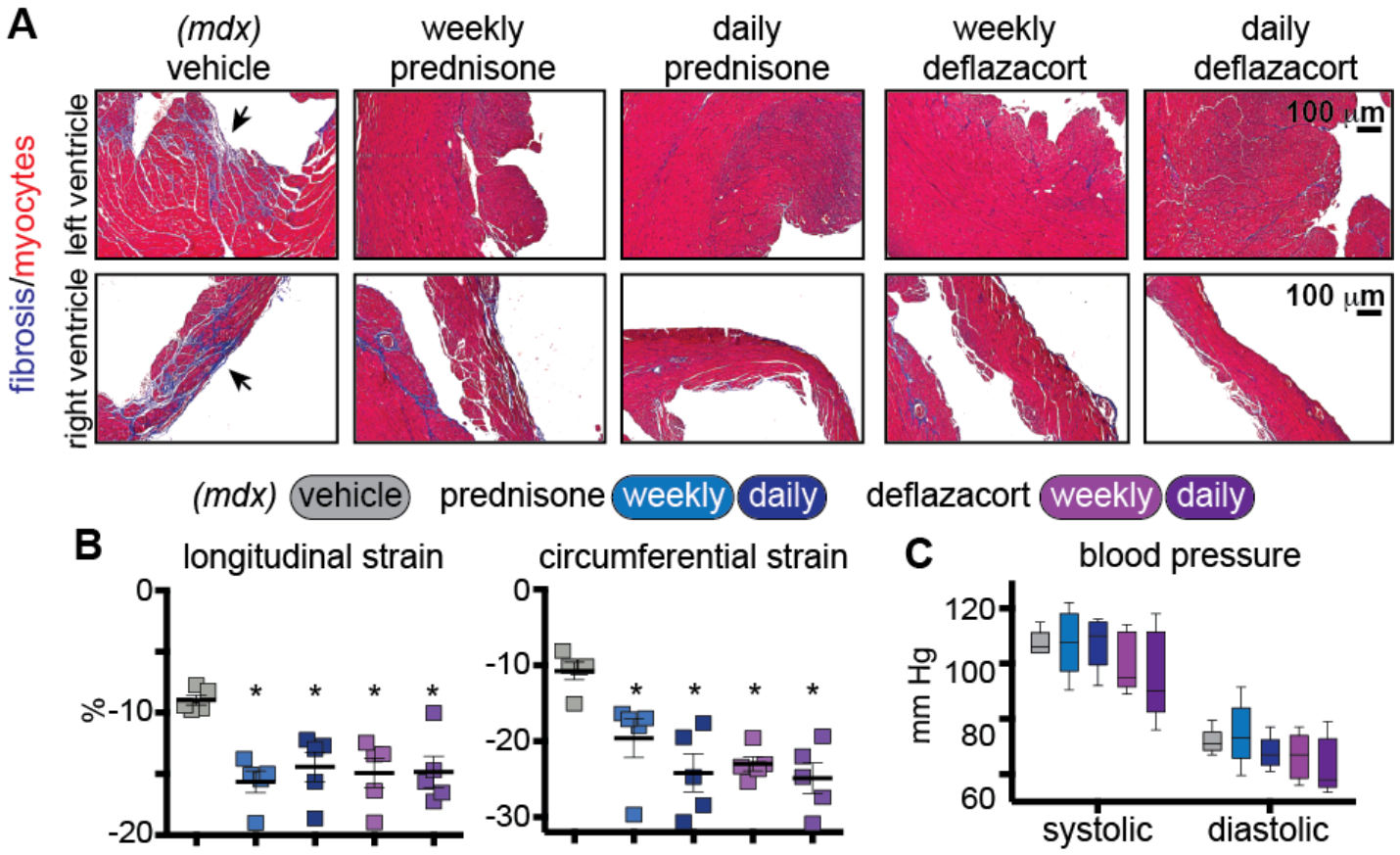

Supplementary Figure 5. Steroid regimens comparably reduce fibrosis and strain in mdx hearts. A) Ventricle wall fibrosis (arrows) appeared comparably reduced after all GC treatments in both left and right ventricles (10 replicates). **B)** Global longitudinal and circumferential strain appeared comparably reduced in all steroid-treated *mdx* mice, as compared to vehicle. **C)** No significant changes were recorded in systolic or diastolic peripheral blood pressure (tail cuff). n=5 mice/group. *, P<0.05 vs vehicle, 1-way ANOVA test with Bonferroni multiple comparison; **#**, P<0.05 vs vehicle, 2-way ANOVA test with Bonferroni multiple comparison.

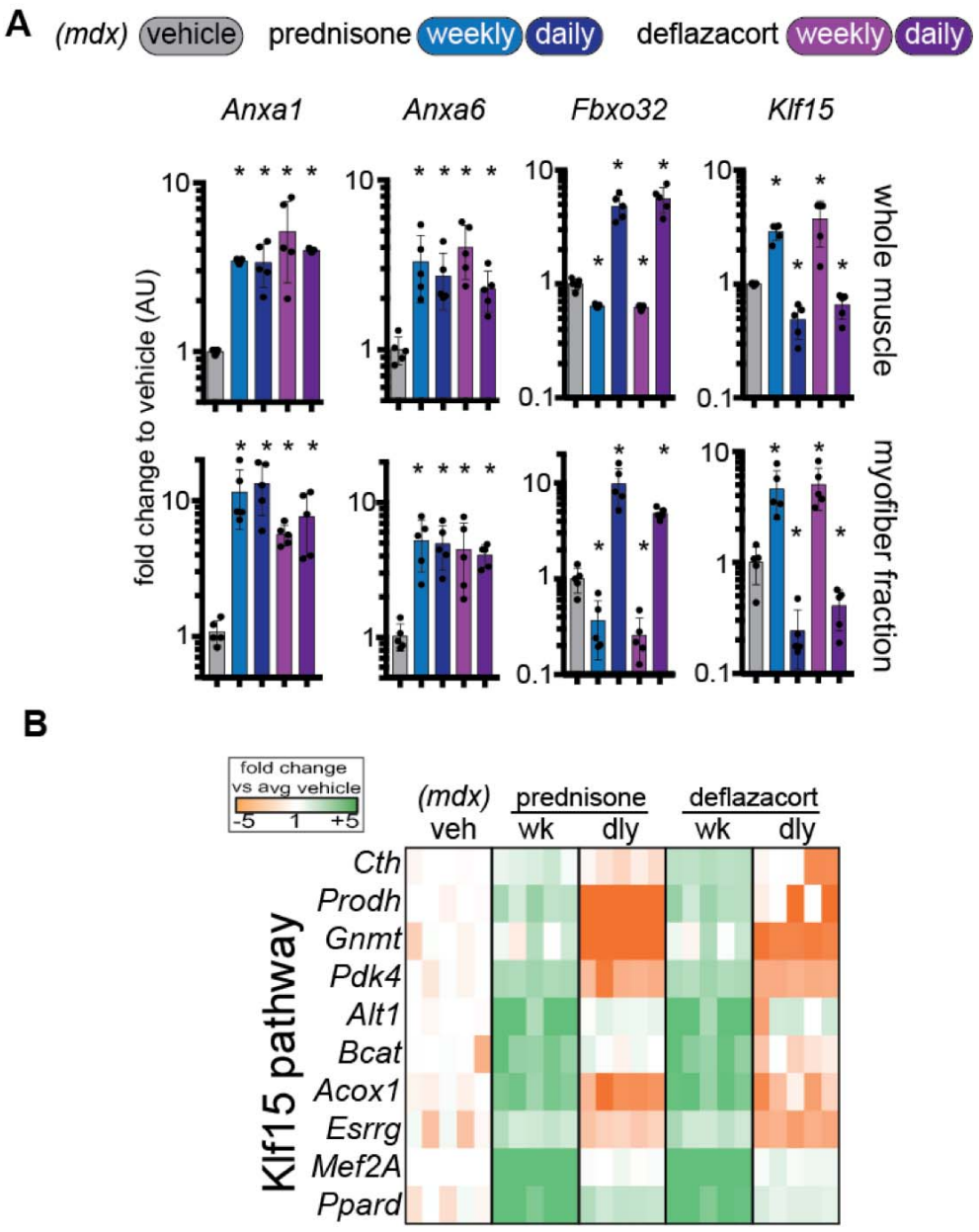

Supplementary Figure 6. Epigenetic and molecular signatures of GC-treated *mdx* muscles. A) qPCR analysis of key candidate genes in whole tissue and myofibers from quadriceps muscles 4 weeks after treatment onset. **B)** Summary heatmap of validating qPCRs for RNA-seq results (quadriceps, whole muscle); orange denotes downregulation, while green upregulation. n=5 mice/group. *, P<0.05 vs vehicle or as indicated, 1-way ANOVA test with Bonferroni multiple comparison.

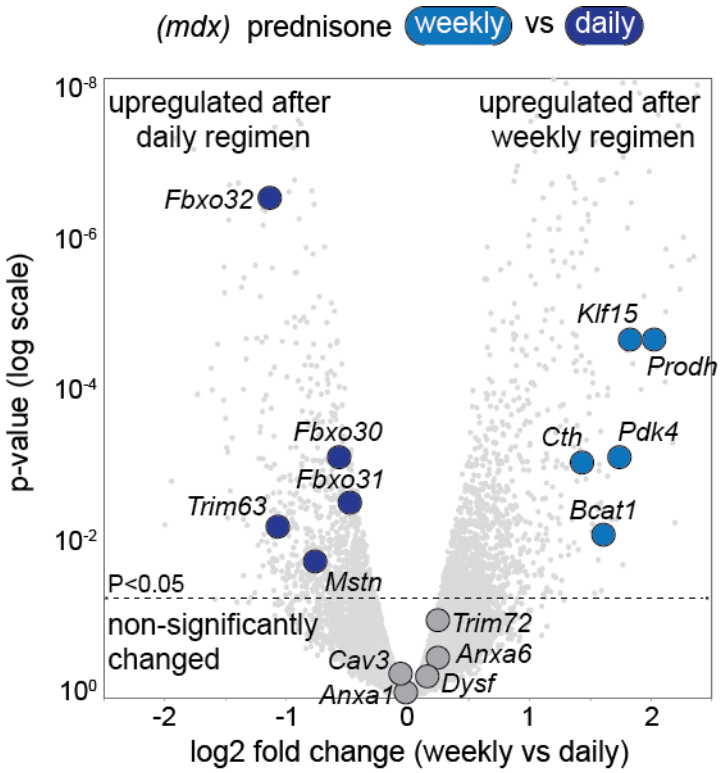

Supplementary Figure 7. GC steroid induced differences between weekly- and daily-dosed muscles. RNAseq analysis from mdx muscle dosed weekly or daily for 4 weeks. Daily steroid dosing was associated with an increase in genes associated with atrophy including *Fbxo32*, *Fbxo30*, *Fbxo31*, *Trim63* and also *Mstn* (myostatin). Weekly steroid dosing promoted the expression of *Klf15* and genes regulated by KLF15. N=5 mice/group; edgeR differential expression test.

SUPPLEMENTAL METHODS

Electroporation, Myofiber Isolation, and Laser Injury.

Methods were described previously in (1) with modifications described in (2). Briefly, the hindlimb footpad was injected with 10µl of hyaluronidase (8units) (Cat #H4272, Sigma, St. Louis, MO). Two hours post injection up to 20µl of 2µg/µl endotoxin free plasmid, 20µl of 10µM miR-mimic, or 20µl of 10µM anti-miR oligonucleotides (Cat. #HMI0553, MSTUD0422; Sigma-Aldrich; St. Louis, MO) was injected into the footpad. Electroporation was conducted by applying 20 pulses, 20 ms in duration/each, at 1Hz, at 100 V/cm. Animals were allowed to recover for a minimum of seven days and not more than ten days after electroporation to avoid examining injured muscle and to allow sufficient time for plasmid expression (3). FDB muscle was removed and individual myofibers were isolated and imaged (2).

Fibers were dissected and laser damaged as described (2, 4, 5). Briefly, fibers were dissociated in 0.2% BSA plus collagenase type II (Cat # 17101, Life Technologies, Grand Island, NY) at 37 degrees in 10% CO_2. After 60 minutes, muscle was triturated. An additional trituration occurred after 120 minutes of digestion. Fibers were then moved to Ringers solution and placed on MatTek confocal microscopy dishes (Cat # P35G-1.5-14-C, MatTek, Ashland MA). After 30 minutes, myofibers were ready for imaging. FM 4-64 dye (T-13320, Molecular Probes, Grand Island, NY) was added to a final concentration of 2.5µm prior to imaging. Fibers were irradiated at room temperature using a Nikon A1R laser scanning confocal equipped with GaSP detectors through a 60x Apo lambda 1.4 NA objective driven by Nikon Elements AR software. We ablated a single pixel set as 120 nm (0.0144 μm^2) using the 405nm laser at 100% power for up to 5 seconds. Images were acquired as follows: one image was acquired prior to damage (preinjury), one image upon laser damage (0 seconds), 10 images every 2 seconds after damage, and then one image every 10 seconds for up to 4 minutes after injury.

Z-stack projections were acquired from approximately 35 consecutive acquisitions with 150 nm interval between each step, using the z-stack rendering built-in tool in NIS-elements AR (Nikon) or ImageJ. FRAP was carried out using tagged annexin proteins on images acquired as stated above in an 85μm^2 region. FRAP measurements were calculated on individual myofibers using ImageJ. Averages were calculated using Prism Graphpad, and values were normalized to the prebleach intensity. Relative fluorescence within the lesion was calculated from images acquired as described above in myofiber isolation and laser damage normalizing each frame to the prebleach intensity. Measurement of the cap diameter was conducted on the diameter perpendicular to the myofiber axis of the nascent annexin cap throughout all frames of analyzed myofiber sequences. All measurements were acquired from myofibers isolated from at least n=3 mice, n≥10 myofibers per mouse. Statistical analysis used Prism Graphpad and a two-way ANOVA; error bars represent the standard error of the mean.

Quality control for myofibers selected for laser ablation was based a number of characteristics. Globally, only myofibers adherent to the MatTek dish from end to end were used and this was to prevent movement during and after laser ablation. Imaged fibers were required to have intact sarcomeres visible in brightfield and the sarcolemma itself was required to be devoid of tears or ruptures induced during the isolation protocol. The region of the myofiber selected for damage was required to be linear without visible deformation including twists or bends in the membrane. Laser ablation was applied to areas without nuclei.

Echocardiography. Cardiac function was assessed by echocardiography was conducted under anesthesia (0.8L/min 1% vaporized isoflurane in 100% O_2) on mice between 2 and 5 days before sacrifice. Echocardiography was performed using a Visual Sonics Vevo 2100 imaging system with an MS550D 22-55 MHz solid-state transducer (FujiFilm, Toronto, ON, Canada). Longitudinal and circumferential strain measurements were calculated using parasternal long-axis and short-axis B-mode recordings of three consecutive cardiac cycles, analyzed by the Vevo Strain software (FujiFilm, Toronto, ON, Canada). Analysis was conducted blinded to treatment group.

Blood pressure monitoring. Twenty-four hours prior to sacrifice, blood pressure was analyzed by CODA system (Cat #CODA-HT-8; Kent Scientific, Torrington, CT) at 7AM on 37°C-warmed heating pad without anesthesia. Analysis was conducted blinded to treatment group (250 measurements per group).

Histology, Immunofluorescence Microscopy (IF) and antibodies. Upon sacrifice, spleen and muscles were dissected. Splenocytes were collected mincing the freshly isolated spleen into a cell suspension and filtering using 100µm and 40µm cell strainers. Excised muscles were immediately frozen in liquid nitrogen, placed in pre-cooled Nalgene cryovials and stored at -80°C, or placed in 10% formaldehyde (Cat #245-684;

Fisher Scientific, Waltham, MA) for histologic processing, or embedded in tissue freezing medium (Cat #TFM-5; Triangle Biomedical Sciences, Durham, NC) for IF analyses. Seven μm sections from the center of paraffin-embedded muscles were stained with hematoxylin and eosin (H&E; cat #12013B, 1070C; Newcomer Supply, Middleton, WI) and Masson's trichrome (Cat #HT-15; Sigma-Aldrich; St. Louis, MO). Ten μm sections from the center of frozen-embedded muscles were collected on the cryostat (chamber, -20°C; sample, -15°C; cat #CM1950; Leica, Wetzlar, Germany). Myofiber CSA quantitation was conducted on 400 myofibers per diaphragm muscle per mouse (2,000 myofibers/group), and 1,200 myofibers per gastrocnemius muscle per mouse (7,200 myofibers/WT group; 6,000 myofibers/mdx group). Diaphragm thickness was conducted on 30 serial diaphragm sections per mouse (150 measurements/mdx group). IF staining was performed with 4% PFA fixation (10 minutes, room temperature), permeabilization with 0.2% Triton (Cat #X-100; Sigma-Aldrich; St. Louis, MO), 1% bovine serum albumin (Cat #A7906; Sigma-Aldrich; St. Louis, MO) PBS (30 minutes, room temperature), blocking in 1% BSA, 10% FBS PBS (30 minutes at room temperature).

Primary myoblast isolation. Primary myoblasts were sorted as $CD56^+$ cells from the mononuclear preparation obtained from *tibialis anterior* muscles, adapting previously reported conditions (6). Briefly, finely minced muscle tissue was digested with 5ml of 0.06% collagenase II (Cat #17101, Life Technologies, Grand Island, NY) solution in basic DMEM (Cat #11995; Life Technologies, Grand Island, NY) for 40 minutes at 37°C while shaking. The mononuclear fraction was then isolated via subsequent filtration through a 100μm- (Cat #352360; Corning, Inc, Corning, NY) and a 40μm cell strainers (Cat # 22363547, Fisher Scientific, Waltham, MA). The heterogeneous primary cell pool was incubated with APC-conjugated anti-CD56 antibody (Cat #FAB7820A; R&D Systems, Minneapolis, MN; 1μl/10^6 cells in 200μl PBS) for 30 minutes at room temperature. Bare and isotype control (rat IgG2A) tubes were processed in parallel. Cells were washed twice in PBS, and $CD56^+$ cells were sorted from the primary pool, gating for the APC^+ fraction at a BD FACSAria 4-Laser flow cytometer (Becton, Dickinson, & Co, Franklin Lakes, NJ). Sorted myoblasts were then cultured in DMEM medium (Cat #11995) supplemented with 20% FBS (Cat #16000), 1% Pen/Strep (Cat #15070; all reagents from Life Technologies, Grand Island, NY), and 5ng/ml FGF2 (Cat #130-093-842; Miltenyi Biotec, Bergisch Gladbach, Germany) and 1% chicken embryo extract (Cat # NC9880840; Fisher Scientific, Waltham, MA). Myoblasts were cultured on collagen-coated (Cat #C9791; Sigma, St. Louis, MO) Nunclon-Delta surface culture vessels (Thermo Fisher Scientific, Waltham, MA). Enrichment for myoblasts in the sorted fraction was confirmed via qPCR analysis of *Pax3/Pax7* expression, and observation of >90% differentiation in myotubes after 10 days of differentiation in serum starvation conditions (DMEM supplemented with 2% horse serum (Cat #16050-122; Life Technologies, Grand Island, NY).

Chromatin immunoprecipitation (ChIP)-qPCR and luciferase assays.
ChIP-qPCR was performed according to previously reported protocol (7) and adjusted conditions (8). Briefly, C2C12 myoblasts were grown and treated between 50 and 80% confluence in DMEM medium (Cat #11995) supplemented with 10% FBS (Cat #16000) and 1% Pen/Strep (Cat #15070; all reagents from Life Technologies, Grand Island, NY). Vehicle, or prednisone, or deflazacort (25μg/ml) were added directly in the growth medium. Twenty-four hours after treatment, one million cells were collected, washed, fixed in 1% PFA and quenched with 0.1375 mmol glycine (Cat #G7126; Sigma-Aldrich; St. Louis, MO). Chromatin was then sonicated for 15 cycles (30 sec, high power; 30 sec pause) in a water bath sonicator set at 4°C (Bioruptor 300; Diagenode, Denville, NJ). Five hundred ng chromatin was used for each pull-down reaction or for the input control samples. Primary antibodies (anti-NR3C1, cat #ab3671, Abcam, Cambridge, MA; anti-FOXO1, cat #2880P, and anti-SRF, cat #5147P, Cell Signaling, Denver, MA) were added at a 1:100 dilution in 300μl volume while shaking overnight at 4°C. Chromatin complexes were precipitated with proteinA/G beads (cat #20421; Thermo Scientific, Waltham, MA). DNA was then de-complexed with proteinase K (cat #19131; Qiagen, Hilden, Germany) at 55°C and purified by means of QIAQuick PCR purification kit (cat #28106; Qiagen, Hilden, Germany). qPCR amplification was conducted as described for gene expression analysis, with a dedicated thermal profile (95°C, 30 sec; 55°C, 30 sec; 72°C, 30 sec; 50 cycles).

RNA-seq analysis. Total RNA was isolated from ~30mg muscle tissue (quadriceps muscles from treated and control *DBA/2J-mdx* male 6 month-old mice) with the RNeasy Protect Mini Kit (Cat #74124; Qiagen, Hilden, Germany) as per manufacturer's instructions. RNA was quantitated at the Qubit fluorometer (Cat #Q33216; Thermo Fisher Scientific, Waltham, MA) and quality-controlled at a 2100 Bioanalyzer (Cat #G2943; Agilent Technologies, Santa Clara, CA). Libraries were prepared from approximately 1μg RNA/sample by means of

TruSeq Stranded Total RNA Library Prep Kit (Cat #RS-122-2203; Illumina, San Diego, CA). Libraries were sequenced through the NextSeq 500 System (high-throughput, paired-end 150bp fragment sequencing; Cat #SY-415-1001; Illumina, San Diego, CA). Raw sequence reads are deposited Reads from each sample were aligned with TopHat v2.1.0 to the mm10 genome assembly (grcm38, version 78) (9). Transcripts were assessed and raw read counts per gene were quantified with HTseq (10). Reads Per Kilobase of transcript per Million mapped reads (RPKM) and fold-changes between groups were calculated using EdgeR from the Bioconductor package (11). Differentially expressed genes were identified by adjusted P-value <0.05. PCA analysis on differentially expressed genes was performed using ClustVis (12). Heatmaps were visualized with GiTools, and unsupervised clustering was conducted using the Manhattan algorithm (average power) (13). Gene ontology (GO) analysis was conducted submitting gene lists to the PANTHER Enrichment Test (release 20160715), built-in analytical tool in the AmiGO2 software suite by the Gene Onthology consortium (14). GO analyses were conducted on the GO Ontology database (version 2016-12-28), using all genes in the *Mus musculus* database as reference list and the GO Biological Process Complete as annotation dataset. Significantly enriched GO terms were identified by adjusted P-value <0.05. GO gene annotations were also used to assist literature mining to compile functional gene lists, e.g. lists of genes associated with sarcolemmal repair, muscle atrophy, and the KLF-15, IGF-1, and NR3C1 (glucocorticoid steroid receptor) pathways.

1. DiFranco M, Quinonez M, Capote J, and Vergara J. DNA transfection of mammalian skeletal muscles using in vivo electroporation. *J Vis Exp.* 200932).
2. Demonbreun AR, and McNally EM. DNA Electroporation, Isolation and Imaging of Myofibers. *J Vis Exp.* 2015106):e53551.
3. Kerr JP, Ziman AP, Mueller AL, Muriel JM, Kleinhans-Welte E, Gumerson JD, Vogel SS, Ward CW, Roche JA, and Bloch RJ. Dysferlin stabilizes stress-induced Ca2+ signaling in the transverse tubule membrane. *Proc Natl Acad Sci U S A.* 2013;110(51):20831-6.
4. Swaggart KA, Demonbreun AR, Vo AH, Swanson KE, Kim EY, Fahrenbach JP, Holley-Cuthrell J, Eskin A, Chen Z, Squire K, et al. Annexin A6 modifies muscular dystrophy by mediating sarcolemmal repair. *Proc Natl Acad Sci U S A.* 2014;111(16):6004-9.
5. Demonbreun AR, Quattrocelli M, Barefield DY, Allen MV, Swanson KE, and McNally EM. An actin-dependent annexin complex mediates plasma membrane repair in muscle. *J Cell Biol.* 2016.
6. Agley CC, Rowlerson AM, Velloso CP, Lazarus NL, and Harridge SD. Isolation and quantitative immunocytochemical characterization of primary myogenic cells and fibroblasts from human skeletal muscle. *J Vis Exp.* 201595):52049.
7. Carey MF, Peterson CL, and Smale ST. Chromatin immunoprecipitation (ChIP). *Cold Spring Harb Protoc.* 2009;2009(9):pdb prot5279.
8. Quattrocelli M, Swinnen M, Giacomazzi G, Camps J, Barthelemy I, Ceccarelli G, Caluwe E, Grosemans H, Thorrez L, Pelizzo G, et al. Mesodermal iPSC-derived progenitor cells functionally regenerate cardiac and skeletal muscle. *J Clin Invest.* 2015;125(12):4463-82.
9. Trapnell C, Pachter L, and Salzberg SL. TopHat: discovering splice junctions with RNA-Seq. *Bioinformatics.* 2009;25(9):1105-11.
10. Anders S, Pyl PT, and Huber W. HTSeq--a Python framework to work with high-throughput sequencing data. *Bioinformatics.* 2015;31(2):166-9.
11. Robinson MD, McCarthy DJ, and Smyth GK. edgeR: a Bioconductor package for differential expression analysis of digital gene expression data. *Bioinformatics.* 2010;26(1):139-40.
12. Metsalu T, and Vilo J. ClustVis: a web tool for visualizing clustering of multivariate data using Principal Component Analysis and heatmap. *Nucleic Acids Res.* 2015;43(W1):W566-70.
13. Perez-Llamas C, and Lopez-Bigas N. Gitools: analysis and visualisation of genomic data using interactive heat-maps. *PLoS One.* 2011;6(5):e19541.
14. Mi H, Muruganujan A, Casagrande JT, and Thomas PD. Large-scale gene function analysis with the PANTHER classification system. *Nat Protoc.* 2013;8(8):1551-66.

Supplementary Table 1. Values from physiological and histopathological analyses in GC-treated *mdx* mice 4 weeks after treatment onset.

		prednisone		deflazacort	
(avg±s.e.m.)	**vehicle**	**weekly**	**daily**	**weekly**	**daily**
grip strength (N)	0.75±0.02	0.95±0.03*	0.61±0.03*	0.90±0.03*	0.60±0.03*
grip strength/body weight (N/g)	0.03±0.004	0.03±0.004	0.02±0.005	0.03±0.006	0.03±0.004

Values related to analyses in *mdx* mice groups 4 weeks after GC treatment onset (n=5 mice/group). *, P<0.05 vs vehicle controls, 1way ANOVA + Bonferroni.

Supplementary Table 2 – Genomic regions encompassing candidate GREs and FOXOs (in bold) and tested for luciferase activity

genomic location (diagram)	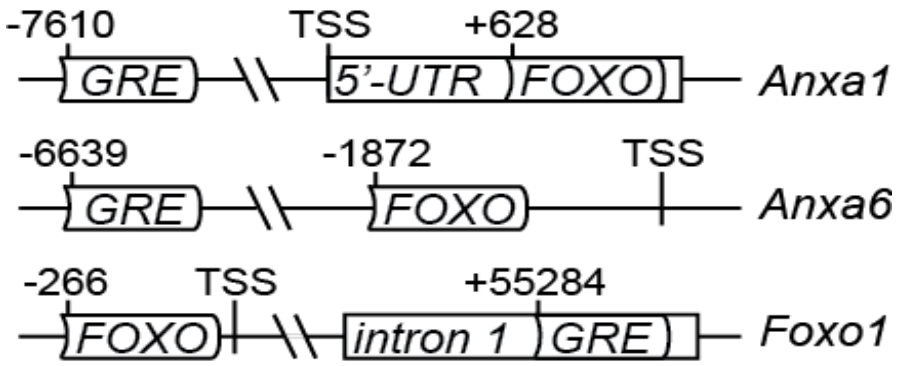
Anxa1GRE	GGGTTTCTCTGTGTAGCCCTGGCTGTCCTGGAACTCACTTTGTAGACCAGGCTGG CCTCGAACTTAGAAATCCGCCTGCCTCTGCCTCCCAAGTGCTGGGATTAAAGGCG TGTGCCACCACGCCCGGCTTAATGCATTTCTTTTATA**AGACACACTGTCA**GCTCTG CTGGTTCATGTTGCA
Anxa1GRE (Δ GRE sequence)	GGGTTTCTCTGTGTAGCCCTGGCTGTCCTGGAACTCACTTTGTAGACCAGGCTGG CCTCGAACTTAGAAATCCGCCTGCCTCTGCCTCCCAAGTGCTGGGATTAAAGGCG TGTGCCACCACGCCCGGCTTAATGCATTTCTTTTATAGCTCTGCTGGTTCATGTTGC A
Anxa1FOXO	GCATTCCGTGGGATGACTTCTCTGACCTCACCCTGGAAAAATCTGCTTTCCCCTTA GGTTTTCAAATGAGCACCAGAAAAGCCTGTCTATGACACAGAGATTATAGGGAG GGGAGGTGGCCACTCCCTGCTTAAATGAGACAAGTAATAAGCGGACCATCTTAAA GTGA**GTAAACA**TAACATTGATTCAAAACGCTAATTAAAAAGGACCACTCGGAGCC TGGGATTCATTTG
Anxa1FOXO (Δ FOXO sequence)	GCATTCCGTGGGATGACTTCTCTGACCTCACCCTGGAAAAATCTGCTTTCCCCTTA GGTTTTCAAATGAGCACCAGAAAAGCCTGTCTATGACACAGAGATTATAGGGAG GGGAGGTGGCCACTCCCTGCTTAAATGAGACAAGTAATAAGCGGACCATCTTAAA GTGATAACATTGATTCAAAACGCTAATTAAAAAGGACCACTCGGAGCCTGGGATT CATTTG
Anxa6GRE	ACGGACCATTCGCAAACAAAAAGAGAGAAAAACTGCCGTGAAACAGCTCAGCAT GTGAGGAGCTCAATAATCTGAGTTGTATTCAGGAACCACAACATGGAAGGAGAG AACCAAGTTC**CACAAGATGTC**CTCTGACCTCCACATGCATACCATGGC
Anxa6GRE (Δ GRE sequence)	ACGGACCATTCGCAAACAAAAAGAGAGAAAAACTGCCGTGAAACAGCTCAGCAT GTGAGGAGCTCAATAATCTGAGTTGTATTCAGGAACCACAACATGGAAGGAGAG AACCAAGTTCCTCTGACCTCCACATGCATACCATGGC
Anxa6FOXO	TGAACGTTTTGCCTGTCTGTAGTATGTACATGCACCACATGTGTGTCCATGTTTAC AGAGGTCAGAAGAGGCCATCAGATCCCTGGAACTGGAGTGACAGAAGGTTGTGA GCCACCCTGTGGGTGCTGTGTCCCCTGCCAGGGCAACAAGTGCTCTTAACCACTG AGCTGCCTCTCCAGGCCTGCAAAA**GTAAACA**TTTTAAAAACATTTCTTTCTACTCA CGCTTATGAGTATATGTCTATCTGGATGAACGTATGCCACACGTGAGCTGGTGTG TTTGGAG
Anxa6FOXO (Δ FOXO sequence)	TGAACGTTTTGCCTGTCTGTAGTATGTACATGCACCACATGTGTGTCCAAGAGGTC AGAAGAGGCCATCAGATCCCTGGAACTGGAGTGACAGAAGGTTGTGAGCCACCC TGTGGGTGCTGTGTCCCCTGCCAGGGCAACAAGTGCTCTTAACCACTGAGCTGCC TCTCCAGGCCTGCAAAA**GTAAACA**TTTTAAAAACATTTCTTTCTACTCACGCTTATG

	AGTATATGTCTATCTGGATGAACGTATGCCACACGTGAGCTGGTGTGTTTGGAG
Foxo1GRE	CTGGAGCATGTTTCTCTTTCCAAATTGAGTGTTGAGAGAATAACAAAGACCAAAT ATTTTACAACACAGACCTTTGAGTTTAACTCTGAAATAGATCTTTTCTTTGCAGTAC TTCTGGTTTTAGTGACACTTACTACTGTGTACTGTCTATTTTTAGCAAACTTTGAAT TCTAAGTAAATAAAAAATTAACTAAATTGGTTTTTAAAATAATACAGATTGTACTT TTTTTTAGTTTCCCATGTCCTAATTGGAAAAGAAGGTCTTACTTGGGATAGAAAT**G CACATTTTGTGC**CAGCCTCTTCTTTGGAATTGGCAAGCGT
Foxo1GRE (Δ GRE sequence)	CTGGAGCATGTTTCTCTTTCCAAATTGAGTGTTGAGAGAATAACAAAGACCAAAT ATTTTACAACACAGACCTTTGAGTTTAACTCTGAAATAGATCTTTTCTTTGCAGTAC TTCTGGTTTTAGTGACACTTACTACTGTGTACTGTCTATTTTTAGCAAACTTTGAAT TCTAAGTAAATAAAAAATTAACTAAATTGGTTTTTAAAATAATACAGATTGTACTT TTTTTTAGTTTCCCATGTCCTAATTGGAAAAGAAGGTCTTACTTGGGATAGAAATC AGCCTCTTCTTTGGAATTGGCAAGCGT
Foxo1FOXO	CAAAACAAACCCCACCGACTTCCCGAGAGCTGCGCGAAGACGCGTGGGCGGAGC GGGCTTGAGTGGAATCCACGAGGCGCCCCACCGCCCACGTCGCGTCCGGGAGCG CGCAGCGGCCCCGCGCCATCCCGGGAGTCAGGGTCTGGGCTCTGCCTGGAGTAC TCGATTGCACTCTGTA**GTAAACA**AAAGTATGGTAGCCGCCTCCACGCCGGTTTGC CTCCTAGCAATCCGATCG
Foxo1FOXO (Δ FOXO sequence)	CAAAACAAACCCCACCGACTTCCCGAGAGCTGCGCGAAGACGCGTGGGCGGAGC GGGCTTGAGTGGAATCCACGAGGCGCCCCACCGCCCACGTCGCGTCCGGGAGCG CGCAGCGGCCCCGCGCCATCCCGGGAGTCAGGGTCTGGGCTCTGCCTGGAGTAC TCGATTGCACTCTGTAAAAGTATGGTAGCCGCCTCCACGCCGGTTTGCCTCCTAGC AATCCGATCG
Klf15GRE	GGTGCGAGAATGGCAGTAACTTTGGGGCCTTCGGACTCCTCAGGGAGAAGACTC TTATTTTGAAGACCGGCCCCCATTCGCCACCCCCGTGATTTGCACGCTGACCCAAT GGCTAGCCCTTGGCCGGCTCTCGGCTTGTTATC**AATTACATGTTGTTCCT**ACAGCC GCTGTGTCCCCGGGAGGATAAACAGCAGGCCTG
Klf15GRE (Δ GRE sequence)	GGTGCGAGAATGGCAGTAACTTTGGGGCCTTCGGACTCCTCAGGGAGAAGACTC TTATTTTGAAGACCGGCCCCCATTCGCCACCCCCGTGATTTGCACGCTGACCCAAT GGCTAGCCCTTGGCCGGCTCTCGGCTTGTTATCACAGCCGCTGTGTCCCCGGGAG GATAAACAGCAGGCCTG

Supplementary Table 3 – Primer list (in gene alphabetical order)

Gene expression primers

mmACOX1 Fw	CTTTGGACCTTCACTTGGGC
mmACOX1 Rev	TTGGGGTCATATGTGGCAGT
mmACTN1 Fw	ATGATTCCCAGCAGACCAAC
mmACTN1 Rev	GAGATGACCTCCAGGAGCAG
mmALT1 Fw	GGGAAGGTGCTAACTCTGGA
mmALT1 Rev	GTCCGGACTGCTCAGAAGAT
mmANXA1 Fw	GGAGAAAGGGGACAGACGTG
mmANXA1 Rev	TGGCACACTTCACGATGGTT
mmANXA6 Fw	TGGCTGCTGAGATCTTGGAAA
mmANXA6 Rev	CGTCCTTGACATCCCCAGAC
mmBCAT2 Fw	GTGTATCCGCCAGCTCATTG
mmBCAT2 Rev	GTCTCCAGGGAAGTAGGAGC
mmCTH Fw	GGGTTTTGAATACAGCCGCT
mmCTH Rev	ATGCCACCCTCCTGAAGTAC
mmESRRG Fw	CTCAAAGTGGGCATGCTGAA
mmESRRG Rev	CCACCAACAAATGCGAGACA
mmFbxo32 Fw	TTGGATGAGAAAAGCGGCAG
mmFbxo32 Rev	TACAGTATCCATGGCGCTCC
mmFOXO1 Fw	AAGAGTTAGTGAGCAGGCTACAT
mmFOXO1 Rev	TTCCCAATGGCACAGTCCTT
mmGNMT Fw	ATCATGCTGGTGGAAGAGGG
mmGNMT Rev	ACTGTTCCCAAGGCAGATGA
mmGZMB Fw	ACAAAGGCAGGGGAGATCAT
mmGZMB Rev	CGAATAAGGAAGCCCCCACA
mmIFNG Fw	CGGCACAGTCATTGAAAGCC
mmIFNG Rev	TGTCACCATCCTTTTGCCAGT
mmIGF1 Fw	CAGAAGTCCCCGTCCCTATC
mmIGF1 Rev	CAAAGGATCCTGCGGTGATG
mmKlf15 Fw	AAATGCACTTTCCCAGGCTG
mmKlf15 Rev	CGGTGCCTTGACAACTCATC
mmMEF2A Fw	AGGAGCTGTGTACGATGCAT
mmMEF2A Rev	TCACAGTCACAGAGCACACT
mmMYH2 Fw	GAGCAAAGATGCAGGGAAAG
mmMYH2 Rev	TAAGGGTTGACGGTGACACA
mmNr0b1 Fw	CTATGTGTGCGGTGAAGAGC
mmNr0b1 Rev	TGGAAGCAGGGCAAGTACTT
mmPAX7 Fw	CGTAAGCAGGCAGGAGCTAA
mmPAX7 Rev	ACTGTGCTGCCTCCATCTTG
mmPDK4 Fw	ATGCCTGTGAAAGAACGTCC
mmPDK4 Rev	TTCGAACTTTGACCAGCGTG
mmPGK Fw	CAAAATGTCGCTTTCCAACAAG
mmPGK Rev	AACGTTGAAGTCCACCCTCATC
mmPOSTN Fw	TATGCTCTGCTGCTGCTGTT
mmPOSTN Rev	CATATAGCCAGGGCAGCATT
mmPPARD Fw	GAACCGCAACAAGTGTCAGT
mmPPARD Rev	GGTAGGCGTTGTAGATGTGC
mmPRODH Fw	GGAAGATCTGAGCCCTGAGG
mmPRODH Rev	TCACACTTGGCTTCATTGGC

ChIP primers

mmANXA1-FOXO Fw	GCATTCCGTGGGATGACTTC
mmANXA1-FOXO Rev	CAAATGAATCCCAGGCTCCG
mmANXA1-GRE Fw	GGGTTTCTCTGTGTAGCCCT
mmANXA1-GRE Rev	TGCAACATGAACCAGCAGAG
mmANXA6-FOXO Fw	TGAACGTTTTGCCTGTCTGT
mmANXA6-FOXO Rev	CTCCAAACACACCAGCTCAC
mmANXA6-GRE Fw	ACGGACCATTCGCAAACAAA
mmANXA6-GRE Rev	GCCATGGTATGCATGTGGAG
mmFoxo1-FOXO Fw	CAAAACAAACCCCACCGACT
mmFoxo1-FOXO Rev	CGATCGGATTGCTAGGAGGC
mmFoxo1-GRE Fw	CTGGAGCATGTTTCTCTTTCCA
mmFoxo1-GRE Rev	ACGCTTGCCAATTCCAAAGA